JOURNAL OF MAGNETIC RESONANCE **124,** 214–217 (1997)
ARTICLE NO. MN967497

An Efficient HN(CA)NH Pulse Scheme for Triple-Resonance 4D Correlation of Sequential Amide Protons and Nitrogens-15 in Deuterated Proteins

TAKAHISA IKEGAMI,* SHIGEO SATO,† MARKUS WÄLCHLI,‡ YOSHIMASA KYOGOKU,† AND MASAHIRO SHIRAKAWA*,§

*School of Bioscience, Nara Institute of Science and Technology, 8916-5 Takayama, Ikoma, Nara, 630-01, Japan; †Institute for Protein Research, Osaka University, 3-2 Yamadaoka, Suita, Osaka, 565, Japan; and ‡Bruker Japan, 3-21-5, Ninomiya, Tsukuba, Ibaraki 305, Japan

Received August 29, 1996

The development of multidimensional triple-resonance NMR techniques has enabled us to study the solution structures of proteins with molecular masses smaller than 25 kDa (*1–3*). Among the experiments, the three-dimensional HN(CA)NNH and H(NCA)NNH methods are extremely beneficial for determining sequential connectivities between neighboring main-chain amide groups (*4*). They have allowed establishment of the direct connectivities between the amide groups of sequentially neighboring residues in a single experiment, while otherwise a combination of two experiments is needed to correlate the amide groups by matching chemical shifts of ^{13}CO and ^{13}Cα resonances with the HNCO–HN(CA)CO and HNCA–HN(CO)CA experiments, respectively. However, the original HN(CA)NNH and H(NCA)NNH experiments are not sensitive enough for medium- and large-sized proteins, owing to the short transverse relaxation time, T_2, of ^{13}Cα spins, as the magnetization transfer passes through the transverse ^{13}Cα spins for 50 ms in these experiments. Since the gyromagnetic ratio of ^{2}H is 6.5 times smaller than that of ^{1}H, the transverse relaxation of ^{13}Cα due to dipolar interactions is reduced by deuteration at the Hα site. Several groups have shown that the effect of scalar relaxation of the second kind for ^{13}Cα caused by the attached deuterons was reduced by deuterium decoupling or heteronuclear cross polarization (*5–8*). Here we present an optimized four-dimensional HN(CA)NH experiment which allowed the detection of 95% of the correlations between the amide proton and nitrogen resonances of the neighboring residues of a 14.7 kDa λ phage Cro V55C mutant protein.

Figure 1 illustrates the pulse sequence employed in the 4D-HN(CA)NH experiment. In contrast to the original 3D experiments by Weisemann and co-workers (*4*), 50% fractional deuteration of the protein and deuterium decoupling were utilized. Also, several parameters have been optimized, i.e., the delays and field strengths of the RF pulses. The coherence flow can be described by

$$\mathrm{H_N}(i) \rightarrow \mathrm{N_H}(i) \rightarrow \begin{cases} \mathrm{C}_\alpha(i) \rightarrow \begin{cases} \mathrm{N_H}(i+1) \rightarrow \mathrm{H_N}(i+1) \\ \mathrm{N_H}(i) \rightarrow \mathrm{H_N}(i) \end{cases} \\ \mathrm{C}_\alpha(i-1) \rightarrow \begin{cases} \mathrm{N_H}(i) \rightarrow \mathrm{H_N}(i) \\ \mathrm{N_H}(i-1) \rightarrow \mathrm{H_N}(i-1). \end{cases} \end{cases}$$

The experiment essentially consists of several INEPT steps for coherence transfer. Suppression of the intense H_2O resonance is achieved with the WATERGATE scheme (*9, 10*). After $^1\mathrm{H_N}(i)$ chemical-shift evolution during t_1, the magnetization is transferred to the attached amide nitrogen, $^{15}\mathrm{N}(i)$, through the INEPT scheme. In the first constant-time period, $2T$, $^{15}\mathrm{N}(i)$ chemical-shift evolution occurs during t_2, and the magnetization is relayed to $^{13}\mathrm{C}\alpha(i)$ and $^{13}\mathrm{C}\alpha(i-1)$ by the following ^{15}N and ^{13}Cα $\pi/2$ pulses, via $^1J[^{15}\mathrm{N}(i) - {}^{13}\mathrm{C}\alpha(i)]$ and $^2J[^{15}\mathrm{N}(i) - {}^{13}\mathrm{C}\alpha(i-1)]$ scalar interactions, respectively.

Assuming that the transverse relaxation time of $^{15}\mathrm{N_H}$ spins is 70–120 ms, we chose 24 ms for the delay, $2T$ which was 30 ms in the original pulse scheme (*4*). From time point a to b, continuous-wave deuterium decoupling is applied to remove the $^{13}\mathrm{C}\alpha-{}^2$H coupling. During the period, ϵ, transverse anti-phase $^{13}\mathrm{C}_\alpha$ magnetization with respect to $^{15}\mathrm{N}(i)$ is partly refocused, while the couplings to the ^{15}N spins of the following and preceding residues evolve. Then, the magnetization is transferred to the $^{15}\mathrm{N}(i-1)$ and $^{15}\mathrm{N}(i+1)$ spins by the simultaneous ^{15}N and ^{13}Cα $\pi/2$ pulses after the period, ϵ. At the same time, the unrefocused ^{13}Cα magnetization, which is anti-phase with respect to $^{15}\mathrm{N}(i)$, is transferred back to $^{15}\mathrm{N}(i)$. In the second constant-time evolution period, $2T$, the chemical shifts of $^{15}\mathrm{N}(i-1)$, $^{15}\mathrm{N}(i+1)$, and $^{15}\mathrm{N}(i)$ evolve during t_3. Finally, the magnetization is transferred to the attached amide protons and detected during t_4.

In the final 4D spectrum, two classes of interresidue frequency coordinates are obtained for the F_1, F_2, F_3, and F_4 dimensions, i.e., $^1\mathrm{H_N}(i)$, $^{15}\mathrm{N}(i)$, $^{15}\mathrm{N}(i+1)$, and $^1\mathrm{H_N}(i+1)$, and $^1\mathrm{H_N}(i)$, $^{15}\mathrm{N}(i)$, $^{15}\mathrm{N}(i-1)$, and $^1\mathrm{H_N}(i-1)$, together

§ To whom correspondence should be addressed.

1090-7807/97 $25.00

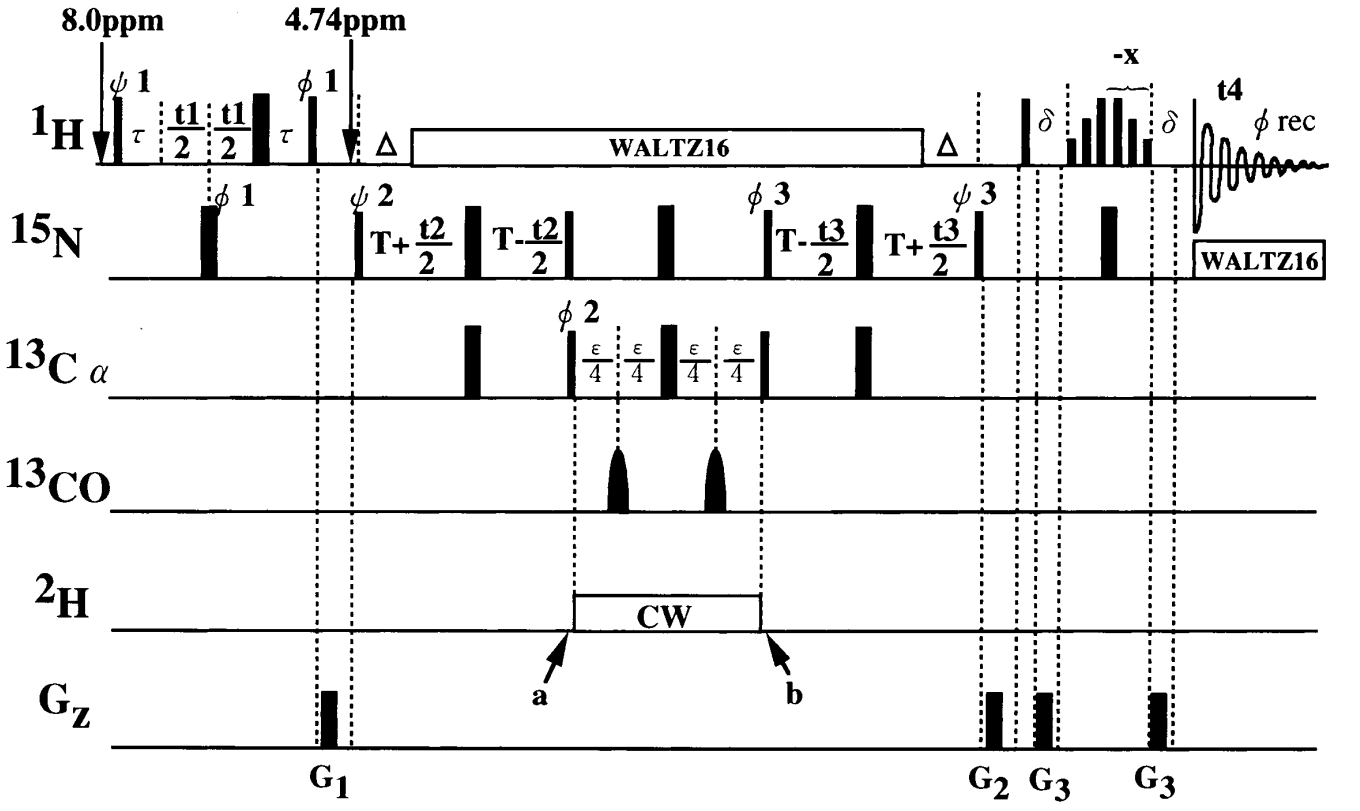

FIG. 1. Pulse scheme for the 4D HN(CA)NH experiment. All narrow pulses correspond to a flip angle of 90°, and wide pulses to 180°, except for the composite WATERGATE 180° pulse train (*10*). Unless indicated otherwise, pulses were applied along the *x* axis. The ^{13}Cα pulses were applied with an RF field strength of 8.77 kHz. The ^{15}N pulses were applied with an RF field strength of 6.35 kHz, except for the WALTZ-16 scheme, where an RF field strength of 1.94 kHz was used. For ^{1}H pulses, an RF field strength of 29.1 kHz was used, except for the WALTZ-16 scheme, where an RF field strength of 6.58 kHz was used. The composite WATERGATE pulse train was a 3—9—19 scheme with a pulse interval of 250 μs (*10*). The ^{1}H carrier was placed at 8.0 ppm for the first three pulses, and then changed to 4.74 ppm. The ^{15}N carrier was placed at 120.0 ppm, and the ^{13}Cα carrier frequency was set at 54.0 ppm. The ^{13}C=O 180° pulses were applied as phase-modulated sin x/x pulses with a duration of 202 μs for the excitation center at 176.0 ppm. The deuterium decoupling was applied as continuous waves using a 1.15 kHz field strength with the carrier at 4.6 ppm. The delays employed were ϵ = 50 ms, τ = 2.3 ms, T = 12 ms, Δ = 5.5 ms, and δ = 1.88 ms (2.3 ms − 1.685 × 250 μs). The phase cycling employed was $\Phi_1 = (y, -y)$; $\Phi_2 = (x, x, -x, -x)$; $\Phi_3 = (x, x, x, x, -x, -x, -x, -x)$; and $\Phi_{rec} = (x, -x, -x, x, -x, x, x, -x)$. Quadrature detection in the F_1, F_2, and F_3 dimensions was achieved by altering ψ_1, ψ_2, and ψ_3, respectively, in the States–TPPI manner (*18*). The durations and strengths of the gradient rectangular pulses were G_1 = (500 μs, 20.1 G/cm), G_2 = (500 μs, −13.4 G/cm), and G_3 = (700 μs, −26.8 G/cm). The recovery time after each gradient pulse was 400 μs.

with intraresidue coordinates $^1H_N(i)$, $^{15}N(i)$, $^{15}N(i)$, and $^1H_N(i)$, respectively. With the delay, ϵ, set at 50 ms, the intensities of interresidue cross peaks are maximum, and those of intraresidue diagonal peaks are smaller (*4*).

The coupling between $^{13}C\alpha$ and $^{13}C\beta$[$^1J(^{13}C\alpha - {}^{13}C\beta) = 35$ Hz], which is active during the period, ϵ, causes a 30% reduction of the signal intensity, since $\cos(\pi J\epsilon)$ was calculated to be 0.7. WALTZ-16 proton decoupling is applied to remove the $^{13}C\alpha - {}^1H\alpha$ coupling and $^{15}N - {}^1H_N$ coupling, instead of the π-pulses or the DANTE pulse trains in the original pulse scheme (*4*).

The 4D-HN(CA)NH experiment was performed for a sample containing 2.0 m*M* λ phage Cro V55C mutant protein, which is a 14.7 kDa protein as a dimer and is cross linked by a disulfide bond, uniformly labeled with ^{15}N, ^{13}C, and ^{2}H (*11*). Fifty percent random ^{2}H labeling was achieved by culturing *E. coli* cells, TG1, harboring overexpression plasmids in the M9 medium of a 50% D_2O/50% H_2O solution containing [$^{13}C_6$]$_D$−glucose (1.0 g/L) and $^{15}NH_4Cl$ (0.5 g/L) as the sole carbon and nitrogen sources, respectively. The NMR measurements were conducted with a Bruker DMX-500 spectrometer with four RF channels, at 37°C and pH 5.9.

Figure 2 shows six (F_1, F_2) cross sections through the 4D-HN(CA)NH spectrum, at the $^{15}N(F_3)$ and $^1H(F_4)$ chemical shifts from Lys^{21} to Tyr^{26}, illustrating the sequential (^{1}H, ^{15}N) → (^{1}H, ^{15}N) J connectivities. Stronger cross peaks, which correspond to interresidue correlations, $^1H_N(i + 1)$, $^{15}N(i + 1)$, $^{15}N(i)$, $^1H_N(i)$, and $^1H_N(i - 1)$, $^{15}N(i - 1)$, $^{15}N(i)$, $^1H_N(i)$, and weaker diagonal peaks, which corre-

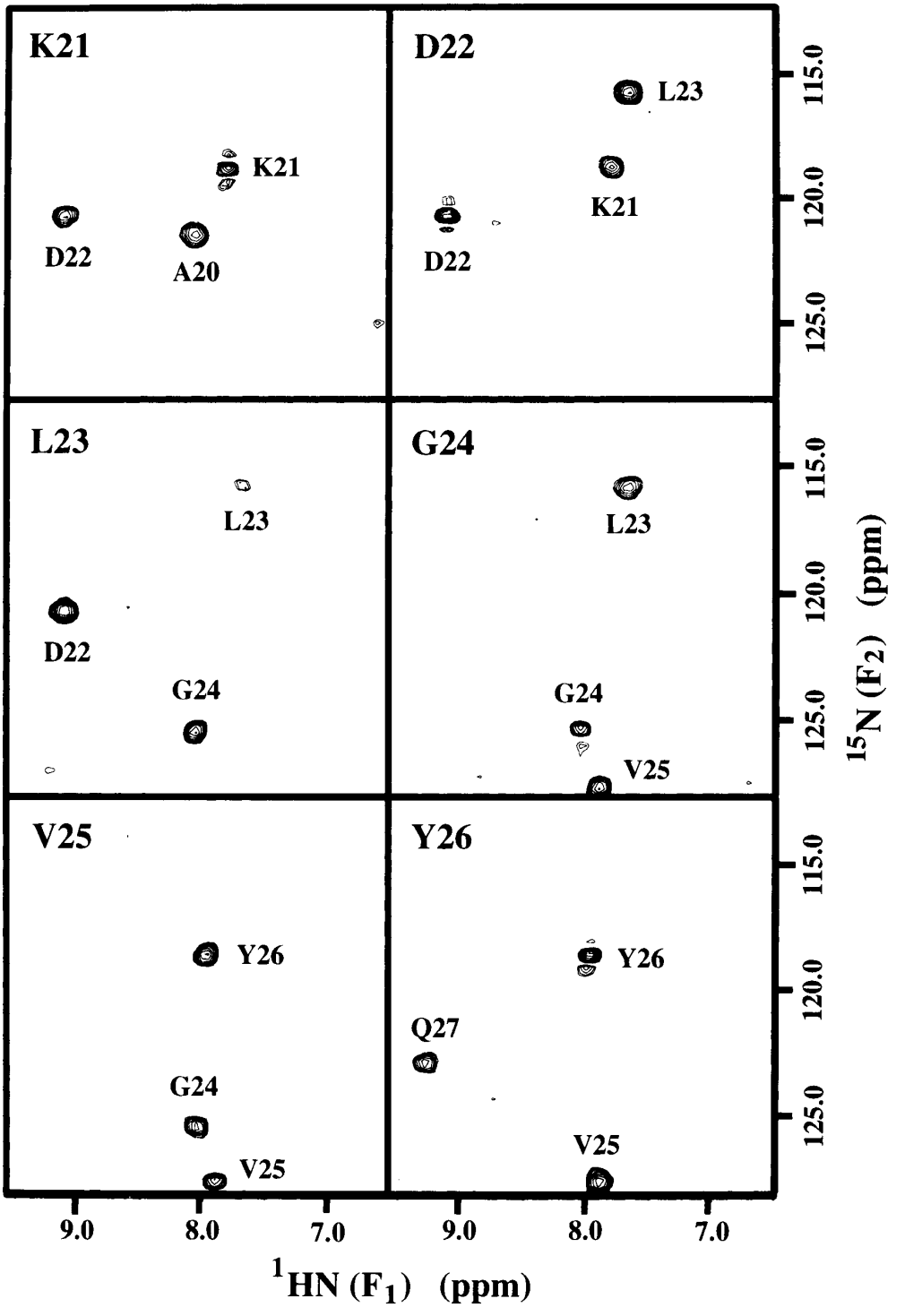

FIG. 2. Six $^{1}H_N(F_1) - {}^{15}N(F_2)$ cross sections, at the $^{15}N(F_3)$ and $^{1}H_N(F_4)$ chemical shifts from Lys^{21} to Tyr^{26}, through the 4D HN(CA)NH spectrum of λ phage Cro V55C mutant protein. The spectrum was recorded with a Bruker DMX-500 spectrometer equipped with four channels for ^{1}H, ^{15}N, ^{13}C, and ^{2}H, and self-shielded triple-axis gradient coils, with a 2.0 m*M* solution of randomly $^{2}H/^{13}C/^{15}N$-labeled protein (50% ^{2}H), 10 m*M* KH_2PO_4–K_2HPO_4 and 25 m*M* KCl, in 10% D_2O/90% H_2O at pH 5.9, 37°C. The data for $13(F_1) \times 15(F_2) \times 15(F_3) \times 512(F_4)$ complex points were acquired in 4.9 days (118 h), giving maximum acquisition times of 8.19 ms (t_1), 18.75 ms (t_2), 18.75 ms (t_3), and 63.9 ms (t_4). Eight scans were accumulated for each FID. The repetition delay was set at 2.14 s (including the duration of the acquisition period). The spectrum was processed using the ''NMRPipe'' suit of programs provided by Delaglio (*19*). In the F_4 dimension, the data were subjected to a cosine-squared apodization followed by Fourier transformation and phasing. Only the amide region of the ^{1}H (F_4) dimension (6.0–10.5 ppm) was used for further processing. The data were doubled by mirror-image linear prediction in the F_2 and F_3 dimensions, and by linear prediction in the F_1 dimension, respectively, giving a final spectrum of $64(F_1) \times 64(F_2) \times 64(F_3) \times 289(F_4)$. Analysis of the spectrum was carried out with the ''Pipp'' suit of programs developed by Garrett (*20*).

spond to intraresidue correlations, $^{1}H_{N}(i)$, $^{15}N(i)$, $^{15}N(i)$, $^{1}H_{N}(i)$, were observed. Since the sensitivity of the experiment was excellent, it often gave both interresidue cross peaks for $i - 1$ and $i + 1$ residues, and intraresidue diagonal peaks for i, which made sequential main chain assignments more straightforward.

We identified 59 of the 63 expected intraresidue diagonal peaks (93.7%), and 115 of the 121 expected interresidue cross peaks (95.0%). The residues whose connectivities we could not identify in the present 4D experiment were located in the N-terminal or C-terminal part of the protein. We also could not obtain the connectivities for these residues in a series of other triple-resonance experiments, i.e., CBCA(-CO)NH, CBCANH, HNCO, and HN(CA)CO, probably owing to chemical exchanges.

During the optimization procedure in the preliminary 1D experiment, we found that changing of the 2T delay to 24 ms (30 ms in the original experiments) caused approximately 10% sensitivity improvement. We also found that application of the WALTZ-16 proton-decoupling scheme gave roughly 25% sensitivity improvement, in comparison to the original scheme where π pulses and DANTE pulse trains were employed (*4*). In addition, incorporation of the WATERGATE scheme effectively eliminated the intense H_2O signal, allowing a larger receiver gain in the experiment.

The sensitivity of the experiment could be further improved by removing the scalar coupling of $^{13}C\alpha$ spins to $^{13}C\beta$ spins during the delay, ϵ. This could be achieved by selective decoupling of $^{13}C\beta$ by applying selective decoupling pulse schemes such as WURST (*12, 13*) or Chirp (*14*), or by replacing the 180° $^{13}C\alpha$ pulse in the middle of the delay, ϵ, with a $^{13}C\alpha$ selective pulse such as r-SNOB (*15*) or the G3-cosine modulated pulse cascade (*16, 17*). The sensitivity would also be improved by the higher deuterium enrichment at the Hα site.

In this Note, we have presented an optimized pulse sequence for the 4D-HN(CA)NH experiment applied to a 50% deuterated protein sample. With the combination of perdeuteration of proteins and the deuterium decoupling scheme, the experiment was shown to be quite sensitive and gave a high quality four-dimensional NMR spectrum for a 14.7 kDa protein with a recording time of 4.9 days. Because the chemical shifts of amide protons and amide nitrogens often give the best dispersion among the nuclei in the main chains of proteins, the pulse scheme can be utilized quite effectively for the main-chain assignments of ^{15}N-, ^{13}C-, and ^{2}H-labeled proteins.

ACKNOWLEDGMENTS

This work was supported by Grants-in-Aid for Scientific Research on Priority Areas (No. 06276102) (M.S.) and Specially Promoted Research (No. 05101004) (Y.K.) from the Ministry of Education, Science and Culture of Japan. M.S. is partly supported by Ciba-Geigy Foundation (Japan) for the Promotion of Science. We thank Dr. Dan Garrett and Frank Delaglio for the use of their programs for NMR data analysis and processing.

REFERENCES

1. M. Ikura, L. E. Kay, and A. Bax, *Biochemistry* **29,** 4659 (1990).
2. L. E. Kay, M. Ikura, R. Tschudin, and A. Bax, *J. Magn. Reson.* **89,** 496 (1990).
3. A. Bax and S. Grzesiek, *Acc. Chem. Res.* **26,** 131 (1993).
4. R. Weisemann, H. Rüterjans, and W. Bermel, *J. Biomol. NMR* **3,** 113 (1993).
5. S. Grzesiek, J. Anglister, H. Ren, and A. Bax, *J. Am. Chem. Soc.* **115,** 4369 (1993).
6. D. M. Kushlan and D. M. LeMaster, *J. Biomol. NMR* **3,** 701 (1993).
7. T. Yamazaki, W. Lee, C. H. Arrowsmith, D. R. Muhandiram, and L. E. Kay, *J. Am. Chem. Soc.* **116,** 11,655 (1994).
8. M. Shirakawa, M. Wälchli, M. Shimizu, and Y. Kyogoku, *J. Biomol. NMR* **5,** 323 (1995).
9. M. Piotto, V. Saudek, and V. Sklenář, *J. Biomol. NMR* **2,** 661 (1992).
10. V. Sklenář, M. Piotto, R. Leppik, and V. Saudek, *J. Magn. Reson. A* **102,** 241 (1993).
11. M. Shirakawa, H. Matsuo, and Y. Kyogoku, *Protein Eng.* **4,** 545 (1991).
12. Ē. Kupče and G. Wagner, *J. Magn. Reson. B* **110,** 309 (1996).
13. H. Matsuo, Ē. Kupče, H. Li, and G. Wagner, *J. Magn. Reson. B* **111,** 194 (1996).
14. J. M. Böhlen and G. Bodenhausen, *J. Magn. Reson. A* **102,** 293 (1993).
15. Ē. Kupče, J. Boyd, and I. D. Campbell, *J. Magn. Reson. B* **106,** 300 (1995).
16. L. Emsley and G. Bodenhausen, *Chem. Phys. Lett.* **165,** 469 (1990).
17. M. A. McCoy, *J. Magn. Reson. B* **107,** 270 (1995).
18. D. Marion, M. Ikura, R. Tschudin, and A. Bax, *J. Magn. Reson.* **85,** 393 (1989).
19. F. Delaglio, S. Grzesiek, G. W. Vuister, G. Zhu, J. Pfeifer, and A. Bax, *J. Biomol. NMR* **6,** 277 (1995).
20. D. S. Garrett, R. Powers, A. M. Gronenborn, and G. M. Clore, *J. Magn. Reson.* **95,** 214 (1991).